The separated electric and magnetic field responses of luminescent bacteria exposed to pulsed microwave irradiation

Catrin F. Williams[1,2*], Gilles M. Geroni[1], Antoine Pirog[1], David Lloyd[2], Jonathan Lees[1], and Adrian Porch[1]

Affiliations

[1]School of Engineering, Cardiff University, Queen's Buildings, Newport Road, Cardiff, CF24 3AA, Wales, UK

[2]School of Biosciences, Cardiff University, Main Building, Cathays Park, Cardiff, CF10 3AT, Wales, UK

*Corresponding author, email: williamscf@cardiff.ac.uk

ABSTRACT

Electromagnetic fields (EMFs) are ubiquitous in the digital world we inhabit, with microwave and millimetre wave sources of non-ionizing radiation employed extensively in electronics and communications, e.g. in mobile phones and Wi-Fi. Indeed, the advent of 5G systems and the "internet of things" is likely to lead to massive densification of wireless networks. Whilst the thermal effects of EMFs on biological systems are well characterised, their putative non-thermal effects remains a controversial subject. Here we use the bioluminescent marine bacterium, *Vibrio fischeri*, to monitor effects of pulsed microwave electromagnetic fields, of nominal frequency 2.5 GHz, on light emission. Separated electric and magnetic field effects were investigated using a resonant microwave cavity, within which the maxima of each field are separated. For pulsed electric field exposure the bacteria gave reproducible responses and recovery in light emission. At the lowest pulsed duty cycle (1.25%) and after short durations (100 ms) of exposure to the electric field at power levels of 4.5 W rms, we observed an initial stimulation of bioluminescence, whereas successive microwave pulses became inhibitory. Much of this behaviour is due to thermal effects, as bacterial light output is very sensitive to the local temperature. Conversely, magnetic field exposure gave no measurable short-term responses even at the highest power levels of 32 W rms. Thus, we were able to detect, de-convolute, and evaluate independently the effects of separated electric and magnetic fields on exposure of a luminescent biological system to microwave irradiation.

MAIN TEXT

Over the last 40 years, a number of insights into the effects of non-ionizing microwave and millimetre-wave radiation on living cells and organisms have been presented, although their interpretation remains controversial[1,2]. Many of these publications concern incident power exposure at levels well below the threshold deemed safe for human treatment regime[3]. The unusual nonlinear responses observed, both in terms of power and frequency dependences, often suggest non-thermal

interaction of electromagnetic fields with biological rhythms in humans[4], living tissue[5] and cells in culture[6], and also with components purified from cells (membranes[7], DNA[8] and enzymes[9]).

To elucidate the extent to which the bioluminescence emitted by washed, non-proliferating bacteria suspended in artificial sea-water can be influenced by pulsed microwave irradiation, 47.4 µl samples in Tygon® E-LFL Non-Bis (2-ethylhexyl) phthalate tubing (of inner diameter 0.9 mm) were employed within a cylindrical aluminium resonant cavity. High spatial separation of the electric (E) and magnetic (H) fields was achieved by exciting the TM_{010} cavity mode. The field distributions are shown schematically in Figure 1 for the case of a circumferential sample tube for magnetic field excitation, and were evaluated by FEM using Poisson Superfish software (Los Alamos National Laboratories[10]). The cavity's inner radius is 4.6 cm, giving a resonant frequency of approximately 2.5 GHz when empty. The inner length is 4.0 cm, which is long enough to ensure high uniformity of the axial E field (i.e. it is ostensibly not affected by the sample holes) but short enough to ensure that the TM_{010} mode is spectrally well-separated[11] from other modes, the next nearest mode beingTM_{110} at 4 GHz. Excitation of the TM_{010} mode is provided by a loop-terminated N-type connector, which couples to the H field around the perimeter of the cavity. The unloaded quality factor *Q* of the empty cavity is measured to be 3000. The coupling loop can be both rotated and moved in and out of the cavity to achieve critical coupling, whereby virtually all incident power is absorbed by the cavity and its contents.

A schematic of the external microwave circuitry is shown in Figure 2. The microwave generator (1, Telemakus TEG27006) provides a single-tone output at a power level of 1 mW rms. The switch (2, Telemakus TES6000-30) directs the signal either to the input of the microwave power amplifier (MPA, 3, Mini-circuits ZHL-30W-262) for cavity excitation "on", or into a 50 Ω matched load for cavity excitation "off". The MPA provides a maximum output power of up to 40 W rms and a power gain of approximately 50 dB. Transmitted and reflected powers are measured using the combination of the directional coupler (4, Mini-circuits ZABDC20-322H) and the precision power

sensors (5, Telemakus TED6000-50). A broadband power sensor (Rhode & Schwarz NRP-Z81) is included for detailed measurement of the power profile of the reflected pulses. The instruments are controlled using National Instruments LabVIEW software, which also records all power readings. The system was arranged to deliver pulsed input power of 4.5 W rms for electric field excitation, or up to 32 W for magnetic field excitation.

Vibrio fischeri bacteria (strain NRRL-B-11177) were cultured in a sea water broth (for 20-24 h at 25°C with 150 rev/min shaking) to stationary phase, the point at which the bioluminescence pathway is activated, as described by Scheerer et al.[12]. Traces of culture medium were removed by washing twice in artificial sea water buffer by centrifugation (MSE, 10 min, 3000 g). Cells were then pumped into the Tygon® tube, which passed through the 5 mm diameter entrance and exit ports in cavity walls. From the field distributions of Figure 1(a) it can be seen that when the tube is run along cavity axis the bacteria are subjected primarily to E field excitation. Conversely, when a section of the tube is run around the circumferential wall (as actually shown in Figure 1) they are subjected primarily to H field excitation. Before exposure, the coupling loop is carefully adjusted to ensure almost critical coupling, whereby the cavity (plus sample load) is impedance matched to the 50 Ω system impedance and all of the input power is delivered to the cavity and its contents. This is confirmed by careful initial measurements of reflected cavity power as a function of frequency measured using a network analyser (Agilent Fieldfox N9923A), before reconnecting to the power delivery system shown in Figure 2. Individual pulse widths were fixed at 100 ms and the duty cycle was varied from 1.25% to 100%. An optical fibre was attached to the sample tube and connected to a photon counting head (Hamamatsu H7467). The photon counts emitted by the bacteria were then measured under microwave excitation using an integration time of 100 ms to reduce measurement noise.

A crucial factor in the design and conclusions of our experiments is the very high degree of E and H field spatial separation produced by simply changing the position of the sample. This

separation can be demonstrated experimentally. When E field excited, the axial sample reduces the resonant frequency from 2.50 GHz to 2.48 GHz (i.e. a reduction of 20 MHz), and the *Q* factor reduces dramatically from 3000 to 50. This shows the very effective coupling to the E field in this sample orientation. When H field excited, the circumferential sample reduces the resonant frequency by only 1.5 MHz, with no measureable effect on *Q*. This indicates that there is negligible E field around the perimeter of the cavity (as expected from Figure 1(b)). Furthermore, any residual electric field is perpendicular to the axis of the sample tube, reducing the E field magnitude within the sea water even further by depolarisation owing to its large relative permittivity ε (around 80 for its real part[13]).

The high degree of field separation is reinforced by the simulated field distribution plots of Figure 1, which shows the perturbed electric and magnetic fields when a circumferential sample is present. In Figure 1 the perturbations have been exaggerated by simulating a much larger diameter tube (of inner diameter 2 mm instead of the practical case of 0.9 mm), placed nearer the axis (3.7 cm from the axis, instead of 4.47 cm in the practical case). As can be seen, the reduction of electric field (Figure 1(a)) within the sample is almost total due to depolarisation, whereas the magnetic field (Figure 1(b)) is almost unaffected. For an axial sample the electric field within the sample is approximately the same of that of the unperturbed cavity, whereas the magnetic field within the sample is enhanced over the unperturbed case (by a factor of approximately $|\varepsilon|$) owing to the increased displacement current within the dielectric sample. The calculated values of the peak E and H fields averaged over the sample volume for the two sample orientations (with rms input powers of 4.5 W for E field excitation and 32 W for H field excitation) are shown in Table 1. These values are for the actual practical case of a 0.9 mm diameter sample, placed on axis or circumferentially a radial distance of 4.47cm from the axis. The electric field magnitude for the axial sample is a factor of x114 larger than for the circumferential sample (i.e. a field intensity E^2 increase of x12900); the magnetic field magnitude for the circumferential sample is a factor of x11.2 larger (i.e. a field intensity H^2 increase of x126). We conclude that any action for the axial sample is driven by the E field, whilst for the circumferential sample is driven by the H field.

The temporal dependence of the measured bioluminescence under microwave exposure in the two sample orientations are shown in Figure 3. Data for the E field excited sample for a 40 s burst of microwave pulses at a power level of 4.5 W rms is shown in the red line plot of Figure 3(a), with microwave pulses of 100 ms duration and 1.25% duty cycle (i.e. six pulses at approximately 8 s intervals). The light output is normalised to the value before exposure, to take into account the natural decay of light output owing to experiments being conducted at different times. The peak E field magnitude was calculated to be 13400 V/m for the axial sample (Table 1). It can be seen that E field excitation leads to an initial enhancement of approximately 12% in light output. Subsequent microwave E field pulses leads to suppression of light output, which diminishes to a greater extent following each 100 ms microwave pulse. These responses of bacterial bioluminescence to the microwave E field are almost certainly due to thermal inhibition, as the sensitivity of bacterial bioluminescence to temperature is well established[14]. The increased suppression of light output with increasing number of pulses is most likely due to the constant increase in sample temperate after each pulse, given that the light output power is a rapidly decreasing function of temperature in the inhibition regime. A surface temperature rise of 4^0C was measured using a thermal imaging camera (Micro-Epsilon) across the sample tube at a power of 4.5 W rms and duty cycle of 1.25%. The equivalent data for H field exposure are also shown in Figure 3(a), for a 10 s burst of microwaves at a power level of 32 W. The peak H field here was calculated to be 183 A/m. Most importantly, no H field effects were measured, even when the power level was increased accordingly. This indicates that, firstly, there is negligible E field present at the sample in this configuration, and secondly that the H field component of the microwave excitation does not measurably influence the bioluminescence intensity at these high power levels. Figure 3(b) shows the repeatability of the E field exposure measurement for three consecutive pulses, for two separate samples. Whilst most of the features of Figure 3 for E field exposure can be explained as having thermal origin (since the bioluminescence is acting as a very sensitive local temperature probe), we are intrigued by the

relatively slow recovery to each of the pulses, and the long term enhancement of light output that cannot be accounted for by increased global temperature alone.

To conclude: our results show the direct bacterial interaction with a microwave electric field with a high degree of suppression of its magnetic component over that of a travelling wave, and *vice versa* for the magnetic field. They indicate the exciting possibilities for further work using this hybrid experimental system to resolve long-standing questions on the extent and importance of non-thermal (i.e. short-pulsed electric field) contributions to widely observed (but unexplained) microwave effects on living tissue, mammalian cells in culture and also with components purified from cells. Of major societal concern, for example, are the possible effects of wireless technologies on child development[15]. In the future we will investigate the frequency dependence of the same perturbations over a broader frequency range and attempt to separate the thermal and non-thermal contributions to the response. We will also elucidate the stage(s) in the bacterial bioluminescence reaction sequence where these perturbations occur, and probe the exact molecular mechanisms involved.

Acknowledgements

We thank Sêr Cymru National Research Network in Advanced Engineering and Materials for a post-doctoral research assistantship (NRN062) to CFW, ENSEIRB (Bordeaux, France) for providing support to A.Pi. for his internship at Cardiff University, Andrew Rankmore (School of Engineering, Cardiff University) for the mechanical construction of the microwave cavity, and Nick Clark (School of Engineering, Cardiff University) for help with the LabVIEW control software. *Vibrio fischeri* strain NRRL-B-11177 was kindly supplied by Dr. Michael H Rayner-Brandes.

References

1. L. Gherardini, G. Ciuti, S. Tognarelli, and C. Cinti, *Int. J. Mol. Sci.* **15**, 5366-5387 (2014).

2. D. T. Pooley, *Q. J. Med.* **103**, 545-554 (2010).

3. World Health Organisation Research Agenda for Radiofrequency Fields. (2010) ISBN 978 92 4 159994 8.
4. N. Halgamuge, *Indian J. Biochem. Biophys.* **50**, 259-265 (2013).
5. Y. Feldman, A. Puzenko, P. Ben Ishai, A. Caduff, and A. Agranat, *Phys. Rev. Lett.* **100**, 128102 (2008).
6. S. Franzelleti, P. Valbones, N. Ciancaglini, C. Biondi, A. Contin, F. Bersani, and E. Fabbri, *Mutat. Res.* **683**, 35-42 (2010).
7. S. Gekle, and R. R. Netz, *J. Phys. Chem. B.* **118,** 4963-4969 (2014).
8. I.Y. Belyaev, Y.D. Alipov, V.S. Sheheglov, and V.N. Lystsov, *A. Naturforch* **47**, 621-627 (1992).
9. Z. Yang, X. Niu, X. Fang, G. Chen, H. Yue, L. Wang, D. Zhao, and Z. Wang, *Molecules* **18**, 5472-5481 (2013).
10. K. Halbach and R. F. Holsinger, *Particle Accelerators* **7**, 213-222 (1976)
11. D.R. Slocombe, A. Porch, E. Bustarret, and O. Williams, *Appl. Phys. Lett.* **102,** 244102 (2013).
12. S. Scheerer, F. Gomez, and D. Lloyd, *J. Micro. Meth.* **67**, 321-329 (2006).
13. T. Meissner, and F.J. Wentz, *IEEE Trans. Geosci. Remote Sensing* **42**, 1836-1849 (2004).
14. D.E. Brown, F.H. Johnson, and D.A. Marsland, *J. Cell. Comp. Physiol.* **20**, 151-168 (1942).
15. L.L. Morgan, S. Kesari, and D.L. Davis, *J. Microscopy Ultrastruct.* **2**, 197-204 (2014).

Tables and Figure Captions

Table 1*: The calculated magnitudes of the axial electric field and circumferential magnetic field averaged over the sample volume, for axial and circumferential samples.*

	Ez (V/m)	Hϕ (A/m)
Tube in axial position (4.5 W)	13400	16.3
Tube in circumferential position (32 W)	118	183

Figure 1**:** *(a) The electric, and (b) magnetic field magnitudes of the TM_{010} mode when perturbed with a circumferential sample, of diameter 2 mm and moved inwards to a radial distance of 3.7 cm from the cavity's axis to exaggerate its perturbation of the fields for illustration purposes. The radial line plots are drawn within the mid-plane, which contains the sample tube.*

Figure 2: *The microwave circuitry used for sample excitations.*

Figure 3: *(a) Effects of microwave exposure to bacterial bioluminescence. The blue line plots (top horizontal axis) are for magnetic field exposure, with 32 W rms power applied for 10 s between the interval 10 – 20 s. Data for H field exposure is shown for a range of duty cycles varying from 1.25% to 100% (different shades of blue), with no measured change in response for all. The red line plot (bottom horizontal axis) is for electric field exposure with 100 ms pulses of microwaves at 4.5 W rms power and 1.25% duty cycle, applied between 20 – 60 s. (b) Detail of the effects of the electric field exposure of (a) for three consecutive pulses (indicated with arrows on (a)), with error bars indicating the standard deviation of two replicates.*

Figure 1

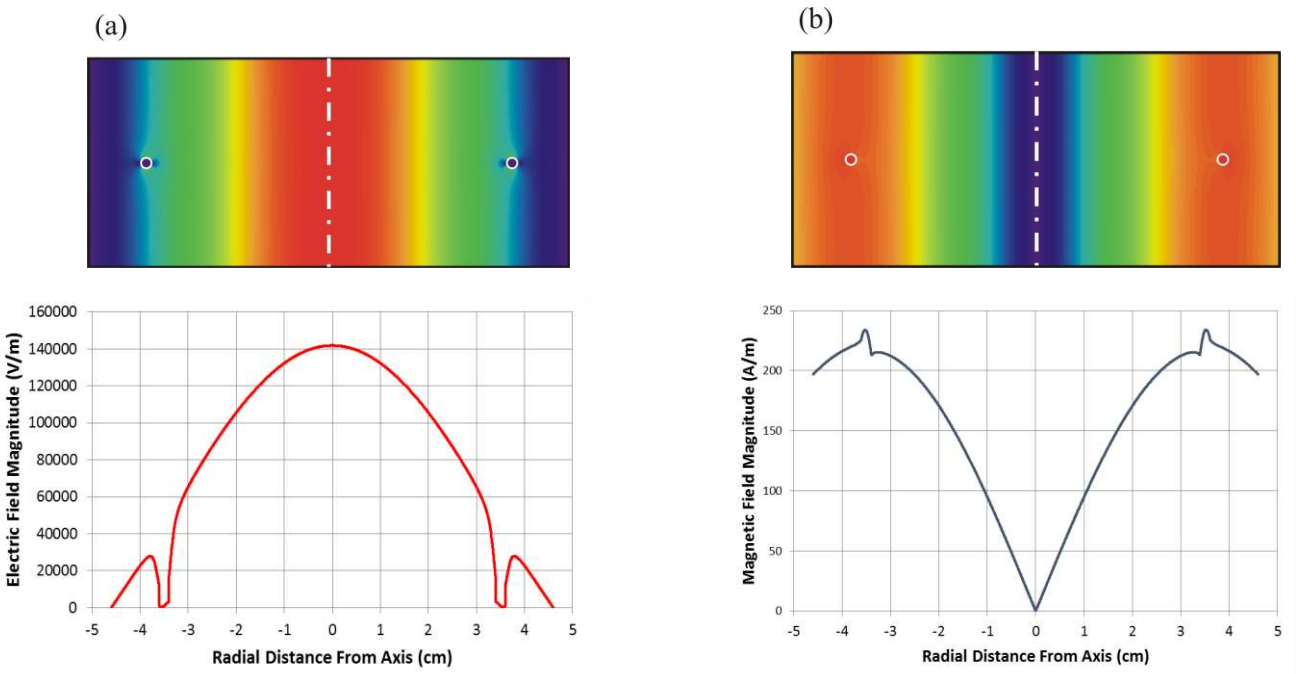
(a)
(b)
Electric Field Magnitude (V/m)
160000
140000
120000
100000
80000
60000
40000
20000
0
-5 -4 -3 -2 -1 0 1 2 3 4 5
Radial Distance From Axis (cm)
Magnetic Field Magnitude (A/m)
250
200
150
100
50
0
-5 -4 -3 -2 -1 0 1 2 3 4 5
Radial Distance From Axis (cm)

Figure 2

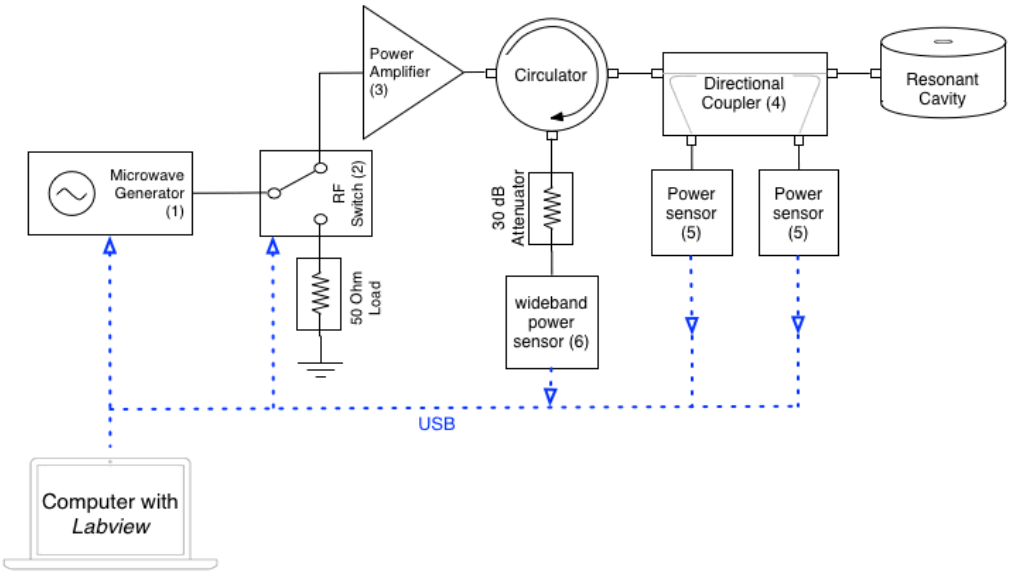
Power Amplifier (3)
Circulator
Directional Coupler (4)
Resonant Cavity
Microwave Generator (1)
RF Switch (2)
30 dB Attenuator
Power sensor (5)
Power sensor (5)
50 Ohm Load
wideband power sensor (6)
USB
Computer with Labview

Figure 3

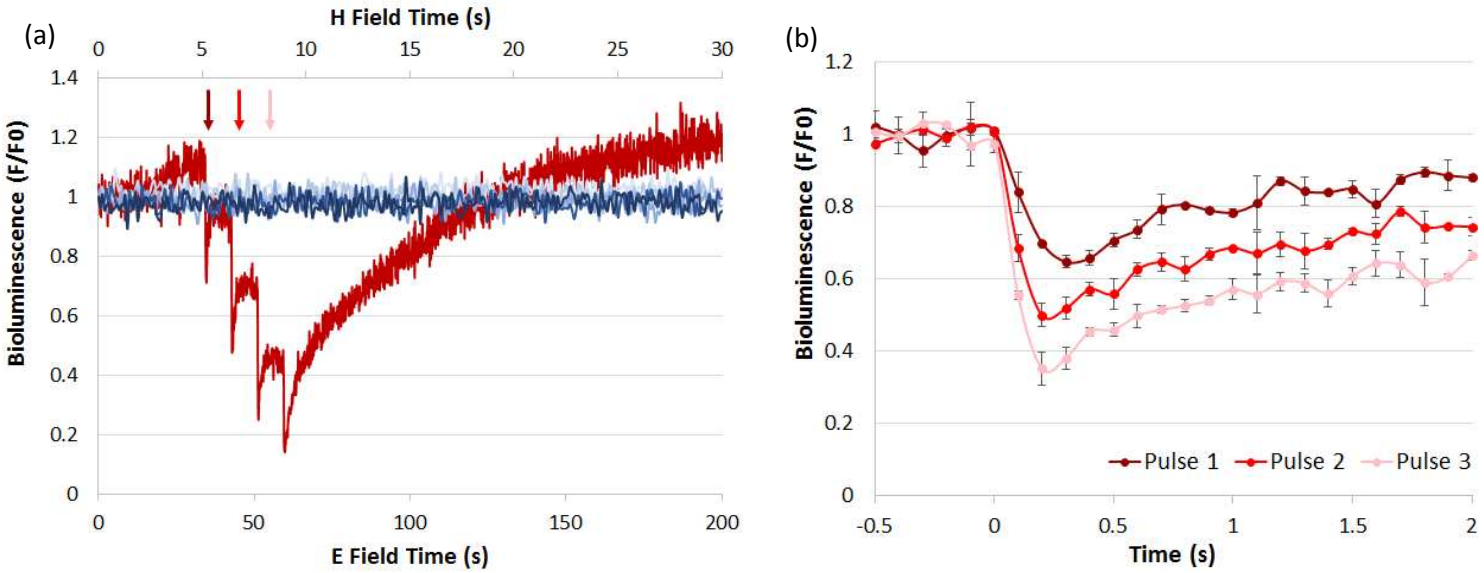
(a)
H Field Time (s)
0
5
10
15
20
25
30
Bioluminescence (F/F0)
1.4
1.2
1
0.8
0.6
0.4
0.2
0
0
50
100
150
200
E Field Time (s)
(b)
Bioluminescence (F/F0)
1.2
1
0.8
0.6
0.4
0.2
0
-0.5
0
0.5
1
1.5
2
Time (s)
Pulse 1
Pulse 2
Pulse 3